SLAC-PUB-10424
April 2004

COSMOLOGICAL FINAL FOCUS SYSTEMS

JOHN IRWIN AND MARINA SHMAKOVA
SLAC, Stanford University, Stanford, CA 94309

We develop the many striking parallels between the dynamics of light streams from distant galaxies and particle beams in accelerator final focus systems. Notably the deflections of light by mass clumps are identical to the kicks arising from the long-range beam-beam interactions of two counter-rotating particle beams (known as parasitic crossings). These deflections have sextupolar as well as quadrupolar components. We estimate the strength of such distortions for a variety of circumstances and argue that the sextupolar distortions from clumping within clusters may be observable. This possibility is enhanced by the facts that i) the sextupolar distortions of background galaxies is a factor of 5 smaller than the quadrupolar distortion, ii) the angular orientation of the sextupolar and quadrupolar distortions from a mass distribution would be correlated, appearing as a slightly curved image, iii) these effects should be spatially clumped on the sky.

1. Introduction

The dynamics for a light stream from a distant galaxy which is collected by an earth-based telescope is shown to be analogous to the dynamics of a particle beam in a final focus system in an accelerator [1]. The beam emittance is well-defined and is similar to that found in present generation accelerators. The dynamics is well approximated by drifts and thin-lens kicks from clusters of matter. The thin-lens kicks are mathematically identical to the kicks arising from parasitic crossings of beams in accelerators. The usual weak gravitational lensing analysis (for recent review see [2], [3] and references therein) restricts itself to the creation of quadrupole moments in the observed light bundle, but here we propose that the sextupole moments, and even octupole moments, may also be observable if the light stream passes close to a dark matter clump. The clump need only have a mass of 10^9 solar masses. We present the mathematics which determines the map from observed image to the source image, and the relationship

Work supported by the Department of Energy Contract DE-AC03-76SF00515

Stanford Linear Accelerator Center, Stanford University, Stanford, CA 94309

Presented at the Joint 28th ICFA Advanced Beam Dynamics and Advanced and Novel Accelerators Workshop on Quantum Aspects of Beam Physics (QABP03), 1/7/2003 - 1/11/2003, Hiroshima, Japan

of that map to the observed moments of the galaxy images. Finally, we report the beginning of our studies of galaxy images in the Hubble deep fields. The magnitude of background sextupole-moments is a factor of 5 smaller than the background quadrupole moments.

2. Final focus analogy

The dynamics governing the light stream from a distant galaxy collected by an earth-based telescope is analogous to the dynamics of a particle beam for two reasons: the dynamics is governed by a Hamiltonian, and the emittance is small. Paths of photons are determined within general relativity by an action principle $I = \int_1^2 g_{\mu\nu}(x) \frac{dx^\mu}{d\lambda} \frac{dx^\nu}{d\lambda} d\lambda$, hence there is a Langrangian $L = \frac{1}{2} g_{\mu\nu}(x) \frac{dx^\mu}{d\lambda} \frac{dx^\nu}{d\lambda}$, a canonical momentum $p_\mu = g_{\mu\nu}(x) \frac{dx^\nu}{d\lambda}$, and a Hamiltonian $H = \frac{1}{2} g^{\mu\nu}(x) p_\mu p_\nu$, defining the trajectory given by Hamilton's equations $\frac{dx^\mu}{d\lambda} = \frac{\partial H}{\partial p_\mu}; \quad \frac{dp^\mu}{d\lambda} = -\frac{\partial H}{\partial x_\mu}$. Since the metric is changing very slowly with time and the gravitational fields are weak, the Newtonian approximation is adequate $g_{00} = -1 - \phi$. For non-relativistic particles $\frac{d^2 x^i}{dt^2} = -\frac{\partial \phi}{\partial x^i}$. Light ray deflections can be calculated from non-relativistic trajectories by multiplying deflection angles by 2.

The emittance can be calculated at the entrance to the telescope. For a 2 m diameter telescope aperture and a galaxy image that has an rms angular radius of 0.1", the emittance is 0.5 mm-mr (millimeter-milliradians). 1" corresponds to $5 \cdot 10^{-6}$ radians. 0.1" is about 2 "drizzled" pixels in the Hubble deep fields.

Furthermore, the light beam dynamics are similar to those of a final focus system, because the telescope translates arrival angles into position on the focal plane rendering the position on the surface of the collecting aperture irrelevant, i.e. only 2 dimensions of the full 4 dimensional phase space is important for the dynamics. The system can be approximated by a series of drifts and thin-lens kicks because the distance between kicks is the order of 500 Mpc (about 1.5 billion light years) whereas the longitudinal size of the mass distributions giving rise to the light bending is usually smaller than 500 kpc (1.5 million light years)(for review see [4]).

The deflection angles are rarely larger than 10^{-4} radian, so one can integrate along the undeflected trajectory to find the magnitude of the thin-lens kick. At a distance x from a point mass the result is

$$\Delta\left[\frac{dx}{ds}\right]=\frac{2}{c}\int\frac{F_x}{m}=-2\int\limits_{-\infty}^{\infty}\frac{GM}{(x^2+s^2)}\frac{x}{(x^2+s^2)^{1/2}}ds=-\frac{4GM}{x}. \quad (1)$$

This $1/r$ kick is similar to the electric field of a line-charge in electrostatics. The potential function is $2\Phi(r) = 4GM\ \ Ln\,[r]$, which is the Green's function for the 2D Laplace equation, $\nabla^2\Phi(\vec{r}) = 4\pi\,G\,\Sigma(\vec{r}) = 4\pi\,G\int_{-\infty}^{\infty}\rho\,(\vec{r},s)\;ds$. In other words, the situation is identical to the parasitic crossings in beamlines. The factor 2 is inserted to obtain potential for light ray deflections from the potential for non-relativistic particle deflections.

3. Multipole analysis

The $Ln[r]$ potential can be written in Cartesian coordinates as $Ln[r] = Re(Ln[x+iy])$. This is an example of the fact that solutions to $\nabla^2\Phi = 0$ can be written as the real part of an analytic function. We will use a standard complex variable notation, $w = x + iy$. We will assume that the light beam is passing the mass distribution at position (x_0, y_0) and expand about this position to get a multipole expansion for the deflections. For a point mass (or outside a spherically symmetric distribution)

$$Ln\,[w_0+w]=Ln\,[w_0]+Ln\left[1+\frac{w}{w_0}\right]=Const-\sum_{n\geq 1}\frac{1}{n}\left[-\frac{w}{w_0}\right]^n.$$

By also introducing the variable $\bar{w} = x - iy$, and noting that derivative operators can be defined by

$$\frac{\partial}{\partial w}=\frac{1}{2}\left(\frac{\partial}{\partial x}-i\frac{\partial}{\partial y}\right)\equiv\partial \text{ and } \frac{\partial}{\partial\bar{w}}=\frac{1}{2}\left(\frac{\partial}{\partial x}+i\frac{\partial}{\partial y}\right)\equiv\bar{\partial}$$

to correctly give $\frac{\partial}{\partial w}w = \frac{\partial}{\partial \bar{w}}\bar{w} = 1$ and $\frac{\partial}{\partial w}\bar{w} = \frac{\partial}{\partial \bar{w}}w = 0$, we are able to express the horizontal and vertical kicks, given by $\delta x' = -\frac{\partial(2\Phi)}{\partial x}$ and $\delta y' = -\frac{\partial(2\Phi)}{\partial y}$, by the single equation $\delta w' = -2\frac{\partial(2\Phi)}{\partial \bar{w}}$.

Returning to the logarithmic potential we get

$$2\Phi=4MG\,\mathrm{Re}(Ln\,[w_0+w])=-2MG\sum_{n\geq 1}\frac{1}{n}\left\{\left[-\frac{w}{w_0}\right]^n+\left[-\frac{\bar{w}}{\bar{w}_0}\right]^n\right\}+const$$

from which it follows that

$$\delta w'=-2\frac{\partial(2\Phi)}{\partial\bar{w}}=-\frac{4MG}{w_0}\sum_{n\geq 1}\left[-\frac{\bar{w}}{\bar{w}_0}\right]^{n-1}$$

These are the usual multipole kicks (dipole, quadrupole, sextupole, octupole).

A general potential distribution can be written

$$\Phi(w,\bar{w}) = \Phi_0 + \partial\Phi\, w + \bar{\partial}\Phi\, \bar{w} + \tfrac{1}{2}\left[\partial^2\Phi\, w^2 + 2\,\partial\bar{\partial}\Phi\, w\bar{w} + \bar{\partial}^2\Phi\bar{w}^2\right] + \tfrac{1}{3!}\left[\partial^3\Phi\, w^3 + 3\,\partial^2\bar{\partial}\Phi\, w^2\bar{w} + 3\,\partial\bar{\partial}^2\Phi\, w\bar{w}^2 + \bar{\partial}^3\Phi\, \bar{w}^3\right] + \ldots$$

from which we see there are additional kick terms all of which contain

$$\frac{\partial}{\partial w}\frac{\partial}{\partial \bar{w}}\;\Phi = \;\frac{1}{4}\left(\frac{\partial^2}{\partial x^2} + \frac{\partial^2}{\partial y^2}\right)\;\Phi = \;\frac{1}{4}\nabla^2\Phi \;\;=\;\; \pi\, G\, \Sigma(\vec{r}).$$

In other words the additional terms will be zero unless Σ(r) or its derivatives are unequal to zero at the light-path centroid.

4. Multipole kick-strength estimates

In our sample of deep field galaxies, the average angular size of the core of distant galaxies in the Hubble deep field is $\theta_G \approx 0.1$". At a distance of 1000 Mpc, where the light path passes a rich cluster, the footprint size would be about 0.5 kpc. A rich cluster of mass $M_C = 5\cdot 10^{14} M_\odot$ would give a light-beam passing at its edge, at a distance from the center of $r_C = 500$kpc , a dipole kick of strength θ_C^D :

$$\theta_C^D = \frac{4GM_C}{r_C} \approx 30 \text{ arc sec}, \qquad \text{implying} \quad \frac{\theta_C^D}{\theta_G} \approx 300.$$

The strength of the quadrupole kick θ_C^Q would be:

$$\theta_C^Q = \frac{4GM_C}{r_C}\left(\frac{r_G}{r_C}\right) \approx 0.03 \text{ arc sec}, \qquad \text{implying} \quad \frac{\theta_C^Q}{\theta_G} \approx 0.3,$$

and the sextupole kick-strength θ_C^S would be

$$\theta_C^S = \frac{4GM_C}{r_C}\left(\frac{r_G}{r_C}\right)^2 \approx 3\cdot 10^{-5} \text{ arc sec}, \qquad \text{implying} \quad \frac{\theta_C^S}{\theta_G} \approx 3\cdot 10^{-4}.$$

This is a hopelessly small number. On the other hand, if the dark-matter clump had a mass equal to $M_C = 5\cdot 10^{10} M_\odot$ and a light-beam is passing at a much smaller distance from the center of the cluster at $r_C = 5$kpc then the quadrupole kick-strength would be the same but the sextupole kick-strength would be 100 times larger:

$$\theta_C^S = \frac{4GM_C}{r_C}\left(\frac{r_G}{r_C}\right)^2 \approx 3\cdot 10^{-3} \text{ arc sec}, \qquad \text{implying} \quad \frac{\theta_C^S}{\theta_G} \approx 0.03.$$

As we will see later, this is approximately the value of the rms sextupole moments of the background galaxies in the Hubble deep field. One could hope to detect such a kick.

5. Finding kick-strengths from image moments

If the source had no quadrupole or sextupole moment one could easily deduce the strength of the kick that would have produced the measured moment. Let the superscripts S and T designate the source and telescope image, respectively. The condition that the source have no quadrupole moments can be written

$$0 = M_{20}^S \equiv \int w_S^2 \; i_S(w_S, \bar{w}_S) \; dx_S dy_S.$$

We will now change from source variables to telescope variables (the map we can deduce goes from the telescope image to the source, in reverse because both the position and the slope are known at the telescope), $w_S = w_T + a\bar{w}_T$. Under this transformation

$$i_S(w_S, \bar{w}_S) = i_T(w_T(w_S), \bar{w}_T(w_S)) \cdot \begin{vmatrix} \frac{\partial w_T}{\partial w_S} & \frac{\partial \bar{w}_T}{\partial w_S} \\ \frac{\partial w_T}{\partial \bar{w}_S} & \frac{\partial \bar{w}_T}{\partial \bar{w}_S} \end{vmatrix}.$$

We end up with

$$\begin{array}{c} M_{20}^S = \int w_S(w_T, \bar{w}_T)^2 \; i_T(w_T, \bar{w}_T) \; dx_T dy_T \\ = \int \left(w_T + a\bar{w}_T\right)^2 \; i_T(w_T, \bar{w}_T) \; dx_T dy_T \\ = \int \left(w_T^2 + 2a w_T \bar{w}_T + a^2 \bar{w}_T^2\right) \; i_T(w_T, \bar{w}_T) \; dx_T dy_T \\ = M_{20}^T + 2a \; M_{11}^T + a^2 \; M_{02}^T \end{array}.$$

Under the assumption that the original galaxy had no quadrupole moment this can be solved for the map coefficient a

$$a = -\frac{M_{20}}{M_{11}} \frac{1}{1 + \sqrt{1 - \frac{|M_{20}|^2}{M_{11}^2}}} \quad \text{and} \quad a \approx -\frac{M_{20}}{2M_{11}} \quad \text{for} \quad \frac{|M_{20}|}{M_{11}} \ll 1.$$

The coefficient a is related to the kick strength through a geometrical factor $a = \frac{D_{LS}}{D_S} \frac{\theta_C^Q}{\theta_G}$. Here D_{LS} is the distance from the source to the lensing matter and D_S is the distance from the telescope to the source galaxy. The ratio of these distances reflects the fact that the apparent displacement of a point in the image due to a kick at the lens plane will be given by the kick strength time this distance ratio.

Similarly the sextupole strength can be found from

$$0 = M_{30}^S \equiv \int w_S^3 \; i_S(w_S, \bar{w}_S) \; dx_S dy_S,$$

yielding

$$\begin{gathered}
M_{30}^{S} = \int w_S(w_T,\bar{w}_T)^3\; i_T(w_T,\bar{w}_T)\; dx_T dy_T \\
= \int \left(w_T + a\,\bar{w}_T + b\,\bar{w}_T^2\right)^3\; i_T(w_T,\bar{w}_T)\; dx_T dy_T \\
= \int \left(w_T^3 + 3b\,w_T^2\bar{w}_T^2 + 3a\,w_T^2\bar{w}_T + \ldots\right)\; i_T(w_T,\bar{w}_T)\; dx_T dy_T \\
= M_{30}^{T} + 3b\; M_{22}^{T} + 3a\, M_{21}^{T} + \ldots
\end{gathered}$$

For small b and negligible $a \cdot M_{21}$, $b = -\frac{M_{30}}{3M_{22}}$. Note that if M_{21} is non-zero, the quadrupole kick can also create a sextupole moment. Non-zero M_{21} requires symmetry breaking and in general will be much smaller than M_{22}, which is equal to $< r^4 >$. Still with a expected to be much larger than b one must pay attention to the possibility that contributions may arise from a non-zero M_{21}.

6. The Hubble deep fields

We have used the software SExtractor [5] to identify and extract galaxy images from the Hubble deep field. This software requires a number of input decisions that affect which galaxies are selected and how their boundaries are defined. One will end up with noisy boundaries (and noisy sextupole moments) for the images unless thresholds are set to be considerably larger than the noise floor. We have used the factor 10 for this input parameter. There is also a subtlety with the convolution matrix for the filter that determines the footprint. In general, less convolution is better.

The extracted images were transferred to the *Mathematica*(www.wolfram.com) computing environment where we could use the full power of the image processing available there. Figure 1 shows contour plots and 3-D images of two of these galaxies. Such images gave us a sense of what we were looking at, and allowed us, for example, to eliminate all galaxies that had two or more maxima. After filtering we had more than 600 high-z galaxies in our selected sample for each Hubble deep field. We measured the sextupole moments for these galaxies, and found them to be about a factor of 5 smaller than the quadrupole moments: they have a dimensionless rms strength of about bσ=0.03. The rms size of the galaxy is introduced to create the dimensionless measure sought. A cautionary note! Our result for this sextupole strength depends on the threshold setting for galaxy intensity. Nevertheless, the sextupole moments are small, as we had hoped (see Figure 2).

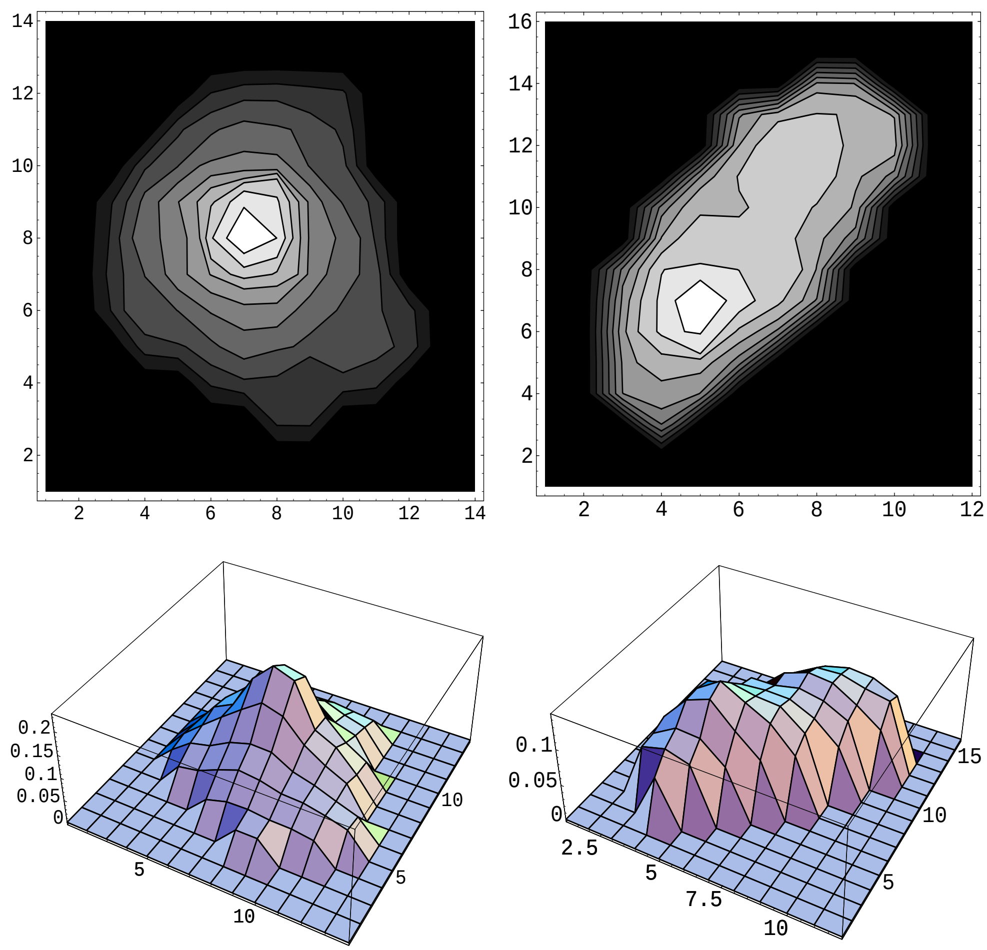

Figure 1. Two galaxy images (contour plots and 3-D plots of surface brightnessfrom the Hubble north field).

7. Correlations and clumping

A careful look at the induced quadrupole and sextupole moments from a kick reveals that together they give a small curvature to the image. This is equivalent to saying that the orientation of the induced sextupolar distortion has its minimum aligned with the minimum of the quadrupolar distortion. We have looked for such a correlation in our galaxy images, and refer to these as "curved" galaxies. We have taken the sample of "curved"

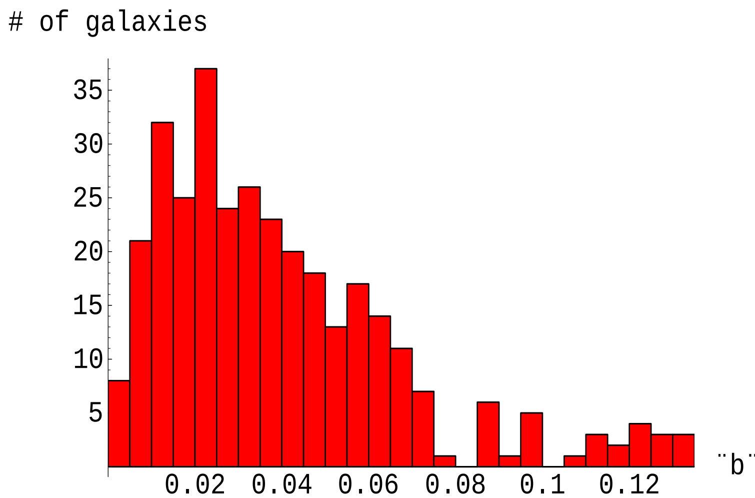

Figure 2. The sextupole strength of faint, z > 0.8 galaxies from Hubble Deep Field (North) data.

galaxies and investigated how these galaxies are arranged on the sky, looking for evidence of clumping. Our conjecture was that if there were clusters of dark matter with sub-clumps of order $10^{10} M_{\odot}$ then the galaxy light paths passing through the cluster might pass near a small clump and become curved. Indeed we have observed statistically significant clumping of curved galaxies in both of the Hubble deep fields. (A random choice of galaxies would give the observed clumping in each field with a probability less than 0.03. Taking the fields together, the probability is less than 1 part per thousand that our result occurs by chance.) However it remains to rule out other possible sources for this clumping. We have determined that if one takes a set of galaxies of a certain slice in z having the same number of members as our curved sample, then clumping is evident as one might expect, since galaxies are known to be clumped. It is also known that high-z galaxies have more complex shapes than low-z galaxies. We are currently investigating whether this correlation can explain our observations.

8. Conclusion (Future plans)

If indeed one can establish that some of the images of distant galaxies are curved because of the presence of small dark matter clumps within larger dark matter clusters, then one might hope to develop a method that would determine the power spectrum of mass structure in the universe on a much smaller angular scale than has been previously possible. To carry out such a program would require the study of larger fields than it is possible with the Hubble, though there are plans for enlarging the Hubble deep field studies. The two fields we have been studying are each about two minutes across, each corresponding to only one part in $2\ 10^7$ of its hemisphere.

Our observations indicate it would be difficult to make these measurements in the presence of atmospheric turbulence. Even a good earth-based point-spread function (PSF) of 0.4" is 6 times larger than the Hubble PSF of 0.07". And the radius of the typical galaxy image we are using is only slightly larger than the Hubble PSF. Fortunately a mission is planned that would do high-resolution lensing from space, known as SNAP (Supernovae Acceleration Probe)[6]. The weak-lensing program for SNAP plans to scan an area of either 300 or 1000 sq. degrees. This would be from $3\ 10^5$ to 10^6 larger than the Hubble deep fields.

We would like to thank Tony Tyson, David Wittman and the Bell-Lab group for encouraging our work and providing us with the orientation and tools needed to get started. We thank Ron Ruth and Pisin Chen for providing support and encouragement for our work at SLAC.

References

1. T. O. Raubenheimer and F. Zimmermann, Rev. Mod. Phys. **72**, 95 (2000).
2. M. Bartelmann and P. Schneider, arXiv:astro-ph/9912508.
3. Y. Mellier, arXiv:astro-ph/9812172.
4. P. J. Peebles, "Principles Of Physical Cosmology," Princeton, USA: Univ. Pr. (1994).
5. E. Bertin and S. Arnouts, Astron. Astrophys. Suppl. Ser.**117**, 393 (1996)
6. J. Rhodes, A. Refregier and R. Massey [the SNAP Collaboration], arXiv:astro-ph/0304417; R. Massey *et al.*, arXiv:astro-ph/0304418; A. Refregier *et al.*, arXiv:astro-ph/0304419.